

Review

# Research Progress of High Dielectric Constant Zirconia-Based Materials for Gate Dielectric Application

Junan Xie <sup>1</sup>, Zhennan Zhu <sup>1</sup>, Hong Tao <sup>2,\*</sup>, Shangxiong Zhou <sup>1</sup>, Zhihao Liang <sup>1</sup>, Zhihang Li <sup>1</sup>, Rihui Yao <sup>1</sup>, Yiping Wang <sup>3</sup>, Honglong Ning <sup>1,\*</sup> and Junbiao Peng <sup>1</sup>

<sup>1</sup> Institute of Polymer Optoelectronic Materials and Devices, State Key Laboratory of Luminescent Materials and Devices, South China University of Technology, Guangzhou 510640, China; 201730294091@mail.scut.edu.cn (J.X.); mszhuzn@mail.scut.edu.cn (Z.Z.); mssxzhou@mail.scut.edu.cn (S.Z.); 201530291443@mail.scut.edu.cn (Z.L.); mslzhscut@mail.scut.edu.cn (Z.L.); yaorihui@scut.edu.cn (R.Y.); psjbpeng@scut.edu.cn (J.P.)

<sup>2</sup> Guangzhou New Vision Opto-Electronic Technology Co., Ltd., Guangzhou 510530, China

<sup>3</sup> State Key Laboratory of Mechanics and Control of Mechanical Structures, Nanjing University of Aeronautics and Astronautics, Nanjing 210016, China; yipingwang@nuaa.edu.cn

\* Correspondence: th@newvision-cn.com (H.T.); ninghl@scut.edu.cn (H.N.)

Received: 7 June 2020; Accepted: 17 July 2020; Published: 20 July 2020



**Abstract:** The high dielectric constant  $ZrO_2$ , as one of the most promising gate dielectric materials for next generation semiconductor device, is expected to be introduced as a new high  $k$  dielectric layer to replace the traditional  $SiO_2$  gate dielectric. The electrical properties of  $ZrO_2$  films prepared by various deposition methods and the main methods to improve their electrical properties are introduced, including doping of nonmetal elements, metal doping design of pseudo-binary alloy system, new stacking structure, coupling with organic materials and utilization of crystalline  $ZrO_2$  as well as optimization of low-temperature solution process. The applications of  $ZrO_2$  and its composite thin film materials in metal oxide semiconductor field effect transistor (MOSFET) and thin film transistors (TFTs) with low power consumption and high performance are prospected.

**Keywords:** high dielectric constant; gate dielectric layer; zirconia; MOSFET; TFT

## 1. Introduction

Since the invention of transistors,  $SiO_2$  has been the most practical choice of gate dielectric materials for field effect transistors. It has several significant advantages, such as high compatibility with silicon chip technology, uniform conformal oxide layer, high interface quality, good thermodynamic stability in contact with Si, etc., which has dominated the silicon microelectronics industry for decades. As the density of integrated circuit increases exponentially, the feature size of metal oxide semiconductor field effect transistor (MOSFET) decreases rapidly, resulting in the thickness of the  $SiO_2$  layer presently used as the gate dielectric becoming thinner. When the feature size of the device continues to shrink to the nanoscale, the ultrathin  $SiO_2$  with low dielectric constant ( $k = 3.9$ ) has reached the physical limit and will eventually be hindered by the inability to reduce the oxide thickness to less than 1.3 nm [1,2]. For ultrathin  $SiO_2$ , the tunneling current caused by the quantum effect will seriously affect the operation of the device. The off-state leakage current will lead to the increase of device power consumption, and even be broken down because of the strong electric field, which makes the gate oxide lose the function of insulation and the device cannot work properly [3]. Therefore, relevant researchers have proposed the application of insulating gates with high dielectric constant (high- $k$ ) materials, which can increase their own physical thickness while ensuring the same channel control ability as ultrathin  $SiO_2$

gate dielectrics, so as to restrain the large leakage current caused by the tunneling effect. As the core component of the flat panel display, the thin film transistor (TFT) device plays an important role in improving the performance of the flat panel display. The properties of the gate dielectric of the TFTs directly affect the performance of the devices. However, the performance of TFTs based on traditional SiO<sub>2</sub> gate dielectric materials cannot meet the requirements of the increasing development of flat panel display. Similar to the metal oxide semiconductor (MOS) devices, TFTs also suffer from tunneling current. Although nitride SiO<sub>2</sub> with improved dielectric constant has been used as the gate dielectric layer in TFTs, it is still unrealistic for continuous scaling in the long term. In order to obtain more compact performance and scaling size of TFTs, the gate dielectric with a high  $k$  value can be used in TFT devices to obtain higher on/off current ratio, lower threshold voltage and lower leakage current, which make it possible to drive TFT at low operating voltage [4,5].

High- $k$  gate dielectric emerged into the market with Intel's new generation 45 nm microprocessors in 2007, in which silicon oxide-based insulator has been replaced by hafnium-based oxides [6]. In recent years, Samsung and Intel have announced the development of the next generation 3D transistors with high  $k$  dielectrics. This review focuses on high- $k$  zirconium-based oxides, which are more abundant in nature also have many excellent properties similar to hafnium-based oxides.

## 2. Zr-Based High- $k$ Dielectrics

A high  $k$  gate dielectric layer provides lower equivalent oxide thickness (EOT) and higher gate capacitance at the desired thickness. The EOT can be calculated as

$$\text{EOT} = \frac{3.9}{K_{\text{hiK}}} t_{\text{hiK}} \quad (1)$$

Here 3.9 is the dielectric constant of SiO<sub>2</sub> and  $K_{\text{hiK}}$  is the dielectric constant of gate oxide and  $t_{\text{hiK}}$  is the thickness of the dielectric layer. Besides, it is vital that the potential barrier at conduction and the valence band offset for Si is greater than 1 eV in order to effectively reduce the leakage currents [7] (Figure 1). A sufficient band offset is required to block the additional current due to Schottky emission and thermal emission as well trap-assisted-tunneling [8]. Electrically active defects are undesirable, which give rise to electronic states in the band gap of the oxide. Charge trapped in defects scatter carriers in the channel and lowers the carrier mobility [7]. The transport performance of the device will be reduced due to impurity defects, remote interface phonons and interface roughness. Hence, it requires additional source–drain ( $V_{\text{DS}}$ ) to source–gate ( $V_{\text{G}}$ ) bias (voltage) as compensation to achieve a desired transistor current ( $I_{\text{DS}}$ ), which in turn increases power consumption [9].

Alternative high- $k$  gate dielectric materials have been investigated, such as HfO<sub>2</sub>, ZrO<sub>2</sub>, Al<sub>2</sub>O<sub>3</sub>, Y<sub>2</sub>O<sub>3</sub> and La<sub>2</sub>O<sub>3</sub>. Among the high  $k$  gate dielectric materials studied at present, zirconia (ZrO<sub>2</sub>) has an appropriate dielectric constant (theoretical value  $k = 25$ ) with a wide band gap (5.8–7.8 eV) and good thermodynamic stability in direct contact with the Si substrate [3,10,11], which is almost similar as HfO<sub>2</sub>. Nevertheless, ZrO<sub>2</sub> can be more easily stabilized in the form of cubic or tetragonal polymorphs with enhanced effective dielectric constant value compared with HfO<sub>2</sub> [12]. In addition, its high melting point (2680 °C), good oxidation resistance, high refractive index (2.15–2.22) [13] and low absorption from near ultraviolet (more than 240 nm) to mid-infrared (below 8 μm) further highlight its technical importance [10,14,15]. It is considered to be one of the most promising high- $k$  dielectric materials and has become a research hotspot. Hence, the purpose of this paper is to introduce the research progress of ZrO<sub>2</sub> and its composite materials as dielectric layers in recent years. Materials and electrical properties of ZrO<sub>2</sub> films prepared by several frequently used deposition methods are described. The main approaches to improve their electrical properties and application prospects in advanced MOSFET and TFT devices are introduced.

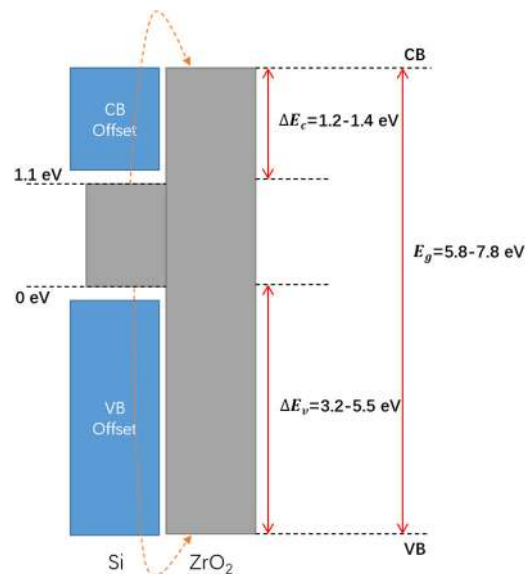


**Figure 1.** Schematic of bandgap and band offsets of  $\text{ZrO}_2$  and carrier injection mechanism in its band states. CB conduction band, VB valence band.

### 3. $\text{ZrO}_2$ Thin Films Deposition

The preparation method of thin films is an important factor affecting the structure and properties of  $\text{ZrO}_2$  gate dielectrics.  $\text{ZrO}_2$  has three kinds of crystal variants, monoclinic crystal (m- $\text{ZrO}_2$ ,  $k = 20$ ), tetragonal crystal (t- $\text{ZrO}_2$ ,  $k = 47$ ) and cubic crystal (c- $\text{ZrO}_2$ ,  $k = 37$ ), while the average  $k$  value of amorphous phase (a- $\text{ZrO}_2$ ) is 22 [10,15,16]. As thin films,  $\text{ZrO}_2$  is usually deposited on the substrate in crystalline form. However, amorphous  $\text{ZrO}_2$  films are preferred for microelectronic devices, because the grain boundaries and defect vacancies in crystalline  $\text{ZrO}_2$  films can cause undesirable increased leakage current as good conductive channels. With the different deposition methods, the  $\text{ZrO}_2$  thin films show different crystal phase structure, which leads to the heterogeneity of the  $k$  value with the film thickness, and changes the device performance. Different deposition temperatures and rates will also affect the properties of  $\text{ZrO}_2$  films by affecting the surface roughness of the films. It can be seen that the improvement of film properties depends on the optimization of the deposition process.

Up to now, many deposition processes have been applied to the preparation of Zr-based high- $k$  gate dielectrics, such as atomic layer deposition (ALD) [17], sol-gel process [18], chemical vapor deposition (CVD) [19], sputtering [20], molecular beam epitaxy (MBE) [21], electron beam evaporation (EBE) [22], pulsed laser deposition (PLD) [23] and so on. The following focused on several main preparation methods.

#### 3.1. Atomic Layer Deposition

The ideal growth process for ALD is by alternately exposing the substrate surface to different precursors, which are strictly separated from each other in the gas phase [24]. The ALD deposition process can be used to achieve large area uniform, dense and non-pinhole thin films, meanwhile doping and interface modification is relatively facile. The size of the film grains can be reduced by a selection of proper precursor chemicals to reduce the processing temperature. It is widely used to precisely control the thickness of each cycle [25].  $\text{ZrCl}_4$  and  $\text{H}_2\text{O}$  are commonly used as reactants (Figure 2). However, hydrogen impurities are introduced from  $\text{H}_2\text{O}$ , which may combine with residual chlorine impurities in the film to form hydrogen chloride and corrode the main metal oxide structure. Therefore, the hydrogen free process is the first choice [26]. Hausmann et al. [27] used highly volatile zirconia alkylamide precursors to realize the preparation of  $\text{ZrO}_2$  films by a smooth, pure and highly conformal low-temperature ALD process. Although it can be deposited at a relatively low temperature, ALD usually requires the equipment to achieve a high vacuum and a low deposition rate ( $0.43 \text{ \AA}/\text{cycle}$ ).

At the same time, impurities (chlorine or iodine from the precursor) can be mixed into the film and reduce the dielectric properties of the film.

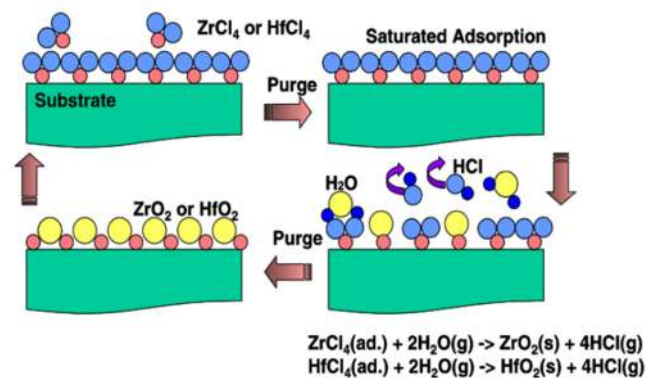


**Figure 2.** Schematic of the cyclic process of atomic layer deposition [7]. Reprinted with permission from [7]; 2015 Elsevier.

### 3.2. Physical Vapor Deposition

For physical vapor deposition (PVD), many methods have been developed to deposit thin films, which are mainly divided into two categories: vacuum evaporation coating and vacuum sputtering coating (as shown in Figure 3). The basic principle is to make the source material evaporate or eject from solid by heating or bombarding the target and finally impact (condense) on the substrate surface [28]. Among them, sputtering is the most commonly used deposition method for  $\text{ZrO}_2$  thin films, by which a good quality of the prepared film, a firm combination with the substrate and a uniform thickness can be achieved [29]. However, sputtered oxides will have plasma-induced damage and difficult to deposited complex shape. The properties of sputtered films mainly depend on the deposition temperature,  $\text{Ar}/\text{O}_2$  ratio, sputtering pressure and post-treatment conditions [30,31]. It was reported [32] that both the oxygen flow rate and post-annealing temperature affect the dielectric constant and surface roughness of the film. In recent years, high-power impulse magnetron sputtering (HiPIMS) systems have been used for high-rate reactive deposition of films (140 nm/min) as a result of the PVD techniques enhancement [13].

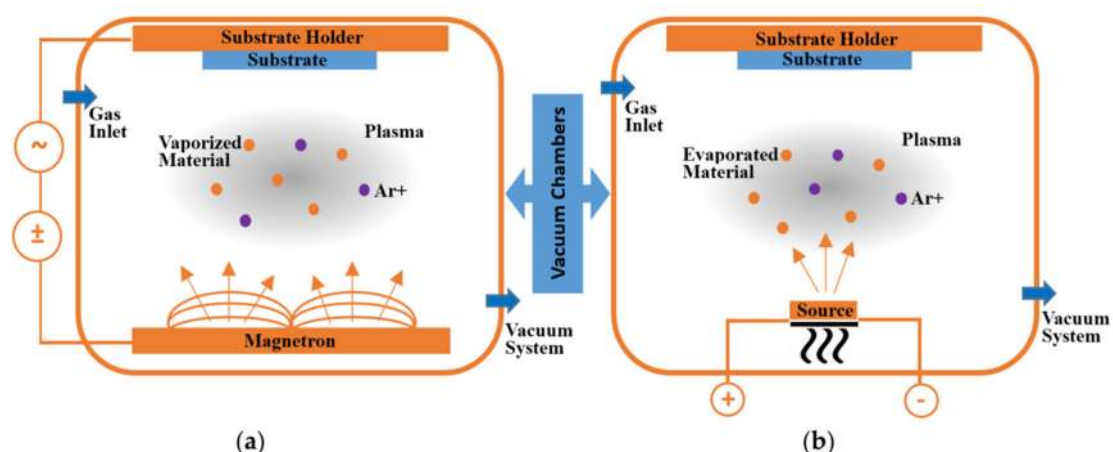


**Figure 3.** Schematic drawing of two conventional physical vapor deposition (PVD) processes: (a) sputtering and (b) evaporating using ionized argon ( $\text{Ar}^+$ ) gas [29].

### 3.3. Chemical Vapor Deposition

Chemical vapor deposition generally has a complex chemical system (Figure 4), which has a relatively low processing temperature and reasonably high deposition rate to produce uniform thin

films with good reproducibility and adhesion. CVD uses a volatile metal compound as a precursor, which is introduced into the chamber and oxidized during deposition onto the substrate. The chemical reactions of precursor species occur both in the gas phase and on the substrate [33]. Reactions can be promoted or initiated by heat (thermal CVD) [19], higher frequency radiation such as UV (photo-assisted CVD) [34] or a plasma (plasma-enhanced CVD) [35]. Moreover, it has capability to mass produce components that are uniformly coated with complex shapes and deposited with good conformal coverage. Furthermore, it has the ability to control the crystal structure, surface morphology and orientation of thin film through well controlled process parameters [33]. A variety of chemical precursors (i.e., halides, hydrides and organometallics) can be flexibly used to deposit target films.  $ZrCl_4$  [33], zirconium acetylacetonate ( $Zr(acac)_4$ ) [36] and  $Zr(OC_4H_9)_4$  [37] are common precursors used as gaseous sources of zirconium to deposit  $ZrO_2$  films. The oxidizing agent can be water vapor, oxygen or binary mixtures, such as  $H_2-O_2$  or  $H_2-CO_2$  [38]. However, for the above CVD process, the high temperature needed to prevent chlorine and carbon-based impurities from contamination usually leads to the formation of highly crystalline thin films with obvious surface roughness [38].

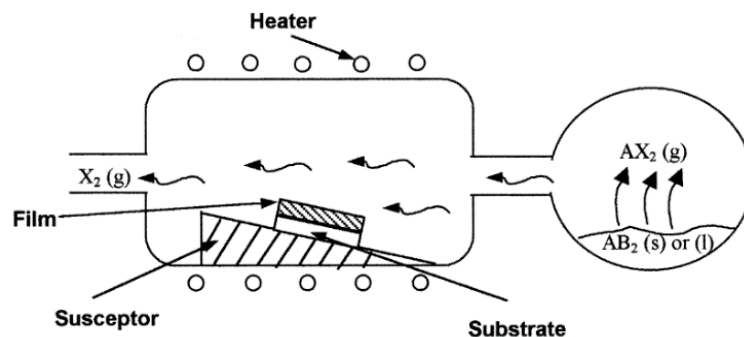


**Figure 4.** Schematic diagram of chemical vapor deposition (CVD) deposition system [38]. Reprinted with permission from [38]; 2003 Elsevier.

### 3.4. Sol–Gel Method

High quality oxide films can be obtained by traditional film preparation methods such as PVD, CVD and ALD, but the equipment requirements and cost of the vacuum treatment are high. Sol–gel chemistry is a method of synthesizing materials through phase transitions from a liquid precursor to a sol (colloidal suspension) and finally to a gel (a network structure) [39], such as spin coating, inkjet printing, spray pyrolysis, dip coating, gravure printing and so on [40]. There are three forms of reaction product, including sol, gel and nanoparticle that can be prepared by controlling the reaction temperature, reaction time, pH value and catalyst, as shown in Figure 5 [40]. By changing the concentration of the precursor solution and deposition period, sol–gel can control the thickness of films with the advantages of low cost, simplicity and high flexibility. Due to the high quality obtained under a mild condition, it is generally used to deposit the relatively thick high  $k$  dielectric layer of TFT [41]. It has also been reported that the sol–gel method was used to prepare ultrathin  $ZrO_2$  films for MOSFET [42,43]. For the preparation of thin films by the solution method, attention should be paid to the molar ratio of the precursor solution and the condition of the post-annealing treatment [44], which are crucial to the properties of the films. Generally speaking, the properties of the films prepared by the solution method are slightly worse than those of other traditional methods such as ALD. However, sol–gel to prepare dense and uniform films that can meet the device requirements with the advantages mentioned above, which is of great significance for mass production in the future, making the solution method a promising film preparation method at present.



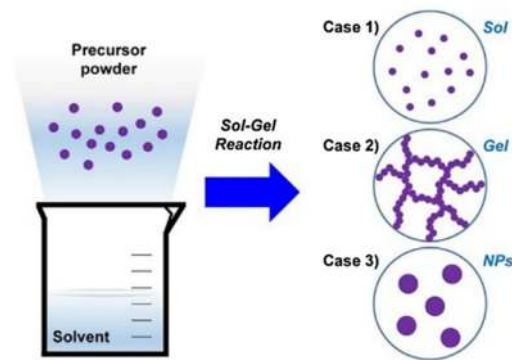


**Figure 5.** Typical sol-gel metal oxide reaction products [40]. Reprinted with permission from [40]; 2017 Elsevier.

#### 4. Methods to Improve the Properties of ZrO<sub>2</sub> Films

Compared with the traditional SiO<sub>2</sub> layer, the low-temperature crystallization of ZrO<sub>2</sub> will lead to the formation of the polycrystalline structure in the annealing process and increase the leakage current. The high  $k$  dielectric has a high rate of oxygen diffusion, resulting in a low  $k$  interfacial layer that is formed inevitably between the silicon substrates in the O<sub>2</sub> ambient, which can increase the EOT. The interfacial properties are also much lower than that of the SiO<sub>2</sub> layer grown on the silicon substrate by thermal oxidation. Furthermore, the coulombic impurity scattering and surface optical phonon scattering cause the problem of carrier mobility loss that limits its application in the future complementary metal oxide semiconductor (CMOS) devices [45]. In this perspective, after the utilization of high dielectric ZrO<sub>2</sub> films, researchers optimized the properties of the derived films by doping other elements or compounds, including the design of pseudo-binary alloy systems by non-metallic elements and metal doping, adoption of new stacking structure, coupling with organic materials and utilization of crystalline ZrO<sub>2</sub> as well as improvement and optimization of the low-temperature solution process.

##### 4.1. Doping of Non-Metallic Elements

Although ZrO<sub>2</sub> has good thermal stability in contact with Si, it is still difficult to prevent the formation of the SiO<sub>2</sub> interfacial layer with low  $k$  and high interface defects due to the diffusion of oxygen during deposition and heat treatment, which usually grows in the post-deposition annealing stage. In the early stage, it is found that the properties of the films have been improved through doping Si, N into ZrO<sub>2</sub>. Lu et al. [46] studied the preparation of (ZrO<sub>2</sub>) <sub>$x$</sub> (SiO<sub>2</sub>)<sub>1- $x$</sub>  silicate (Zr-Si-O) thin films with different compositions on p-Si substrates by pulsed laser deposition. Compared with pure ZrO<sub>2</sub>, Zr-silicate in direct contact with Si has higher crystallization temperature and superior thermal stability [47]. X-ray photoelectron spectroscopy (XPS) analysis shows that the (ZrO<sub>2</sub>)<sub>0.5</sub>(SiO<sub>2</sub>)<sub>0.5</sub> film is still amorphous after rapid annealing in nitrogen at 800 °C for 60 s. Doping more Zr concentration in (Zr-Si-O) silicate film can obtain a higher dielectric constant. However, with the further increase of Zr concentration, obvious phase separation and precipitation of ZrO<sub>2</sub> will occur in Zr-silicate, which will worsen the interface between Si and Zr-silicate [48,49].

Many studies have been devoted to interface engineering solutions that introduce a high-quality oxide or nitride reaction barrier layer with very low defect density between high- $k$  oxide and Si to separate the silicon channel from the dielectric [45,50] (Figure 6a). It can reduce the decrease of carrier mobility due to remote scattering, but at the cost of increasing the thickness of the equivalent oxide. In addition, nitrogen doping in the gate oxide layer is found to be beneficial to improving the thermodynamic properties, effectively reducing the interface layer thickness and leakage current density [35,51,52]. A further decrease of the diffusion coefficient of oxygen in the alloy, thus reduces

the crystallization rate significantly, so that the silicate can withstand the high temperature required by doping activation steps in the MOS process [53].

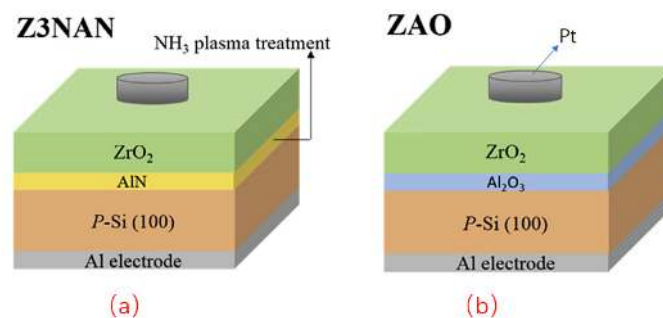


**Figure 6.** Schematic diagram of the (a) Z3NAN and (b) ZAO gate stacks [50]. Reprinted with permission from [50]; 2016 Elsevier.

#### 4.2. Metal Elements Doping

The high bandgap (8.9 eV) of  $\text{Al}_2\text{O}_3$  makes it have good thermodynamic stability with a moderate relative permittivity of 9. Incorporation of  $\text{Al}_2\text{O}_3$  into  $\text{ZrO}_2$  gate dielectrics combines the advantages of constituent dielectrics and markedly increases the crystallization temperature [54], which produce devices with improved performance and stability compared to the pure  $\text{ZrO}_2$  film. In addition, the doping of small-size Al atoms into  $\text{ZrO}_2$  that have greater densification can reduce the oxygen vacancy and smooth the gate dielectric interface [55,56]. Thereby, reducing the interface defects and gate leakage current as well as weakening the carrier mobility reduction effect caused by surface roughness scattering. Liu et al. [57] incorporated  $\text{Al}_2\text{O}_3$  into  $\text{ZrO}_2$  to optimize and adjust its electrical properties such as capacitance and leakage current. Our group also reported a high-k Zr– $\text{AlO}_x$  dielectrics were fabricated by sol–gel spin coating at a low temperature annealing process, which can be applied to the preparation of high performance TFT [58]. By adjusting the  $k$  value of the gate dielectric from 11.3 to an appropriate value (8.1), a reasonable tradeoff is achieved between the gate screening effect on the Coulomb-impurity scattering and the surface optical phonon scattering [57], thus greatly improving the carrier mobility of the device. It has been reported that the mobility of  $\text{Zr}_{0.5}\text{Al}_{0.5}\text{O}_y$  sample was 41% higher than that of the control sample ( $40.6 \text{ cm}^2/\text{V}\cdot\text{s}$ ) [57]. In reference [50,59], it is proposed that  $\text{Al}_2\text{O}_3$  can be used as a transition layer to effectively block the diffusion of oxygen to the matrix and the interfacial reaction, so as to ensure the stability of the Zr–Al interface (Figure 6). Therefore, the quality of the gate dielectric layer can be effectively improved by using  $\text{Al}_2\text{O}_3$  as the buffer layer or doping it into other high  $k$  materials.

In addition to the usual modification of doped Al, rare earth elements such as lanthanum (La) [60], gadolinium (Gd) [61], hafnium (Hf) [62] and yttrium (Y) [63] have also been studied to improve the performance of  $\text{ZrO}_2$  films, which can effectively restrict the formation of low- $k$  silicon oxides and obtain denser gate dielectric films with high-quality interfaces. The overall dielectric constant of pseudo-binary alloys may be lower than that of pure metal oxides, but this compromise is acceptable in order to improve stability. At present, the design of pseudo-binary alloy modified films by doping non-metal or metal elements is a mature way to improve the properties, which is the most promising structure for large-scale application in the industry.

#### 4.3. Coupling with Organic Materials

In recent years, the development of organic–inorganic hybrid thin film materials for dielectric gate applications has aroused great interest of researchers [64]. In theory, organic materials for dielectric gate applications offer a smooth surface and good compatibility, but their low dielectric constant lead to low capacitance [9,65]. On the other hand, the high processing temperature of inorganic dielectric materials with high  $k$  values is not compatible with deposition on flexible plastic substrates required

in flexible electronics [66,67]. Accordingly, the appropriated incorporation of organic and inorganic phases in organic–inorganic hybrid materials, stalwartly bonded at the molecular level, is a new approach to develop dielectric materials with enhanced performance and broad application. However, it is still a challenge to deposit these materials as smooth films at temperatures compatible with flexible plastic substrates. Shang et al. [68] reported the application of bilayer poly (methyl methacrylate) (PMMA)/ZrO<sub>2</sub> gate dielectrics in copper phthalocyanine (CuPc) field effect transistor (FET; Figure 7a). Owing to the deposition of PMMA layers on ZrO<sub>2</sub>, the dielectric leakage is reduced by an order of magnitude compared with single-layer ZrO<sub>2</sub>, resulting in a high-quality interface between organic semiconductors and composite insulators. The device combines the advantages of polymer and high *k* inorganic materials to achieve high mobility and low threshold voltage. It is reported that the typical field-effect mobility of bilayer dielectric field-effect devices is  $5.6 \times 10^{-2} \text{ cm}^2/\text{V}\cdot\text{s}$  and the threshold voltage is 0.8 V [68].

In addition, there are reports on the application of ZrO<sub>2</sub> doped polymer modified thin films in the dielectric gate of metal oxide thin film transistor (MOTFT) [69,70] (Figure 7b) and organic thin film transistor (OTFT) [67,71,72] (Figure 7c). Among them, many of these hybrid materials can be obtained by the sol–gel method, which is a solution, low-temperature process compatible with deposition on large-area substrates. The performance of these hybrid films, including interface quality and dielectric properties, can be adjusted by controlling the content of organic and inorganic components. It can be seen that Zr-based organic hybrid films have great potential applications in a variety of large area printing flexible electronic applications such as displays, sensors and electronic bar codes [66,73].

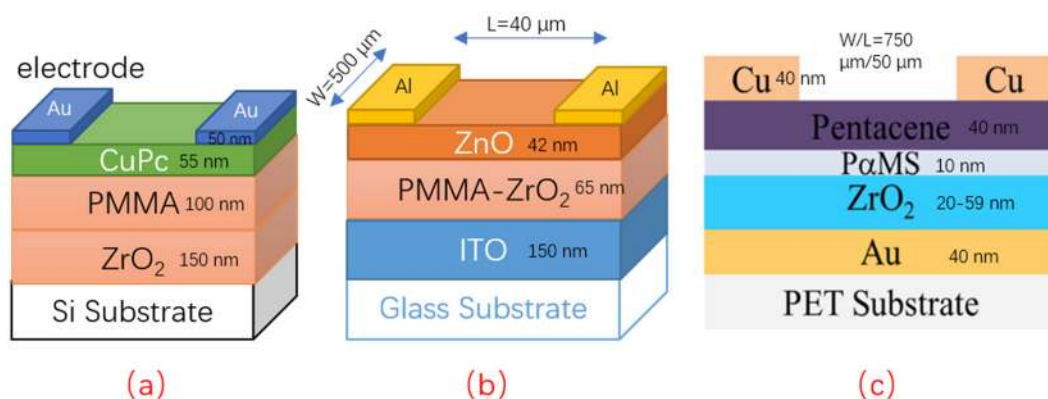


**Figure 7.** (a) Schematic structure and dimensions of the Organic Field Effect Transistors (OFET) with the PMMA/ZrO<sub>2</sub> bilayer as dielectrics [68]; (b) Schematic structure and dimensions of the metal oxide thin film transistor (MOTFT) with a ZnO semiconductor layer and PMMA–ZrO<sub>2</sub> hybrid films as gate dielectric [69]; (c) Schematic structure and dimensions of the organic thin film transistor (OTFT) with the PαMS/ZrO<sub>2</sub> bilayer as dielectrics [72].

#### 4.4. Crystalline ZrO<sub>2</sub> Dielectric

Recently, crystalline ZrO<sub>2</sub> has attracted considerable attention due to the tetragonal (47) and cubic (37) phase of ZrO<sub>2</sub> having a much higher *k* value than amorphous ZrO<sub>2</sub>. However, the grain boundaries may serve as the leakage current paths, which will cause a dramatic leakage current in the dielectric gate layer application. Moreover, the tetragonal and cubic phase of ZrO<sub>2</sub> are only stable in bulk form above 1170 and 2297 °C respectively, which is not suitable for ultra-large-scale integration (ULSI) technology [15,74]. Hereby, reducing the film thickness or grain size or doping impurities such as Si, Ge and La [14,74,75] into the lattice had been exploited to decrease their stable temperatures. The tetragonal/cubic phase of ZrO<sub>2</sub> can be formed by post-metallization annealing (PMA) at a low temperature of 450 °C to provide a high gate oxide dielectric constant [76]. Ge-induced stable ZrO<sub>2</sub> crystals can be formed by co-evaporation of Ge and ZrO<sub>2</sub> or thermally diffused into ZrO<sub>2</sub> films by Ge substrates, thus stabilizing the high-*k* tetragonal phase [75,77–79]. What is more, as a channel



material, Ge has many advantages, such as higher carrier mobility than traditional Si and compatibility with the Si process. In addition, some research [76,80,81] has reported that nitriding can effectively passivate grain boundaries and reduce leakage current density. On the other hand, the thermal stability is enhanced through post-deposition annealing (PDA) treatment at 800 °C (Figure 8) and the hysteresis problem affecting the threshold voltage stability is reduced to the maximum extent.

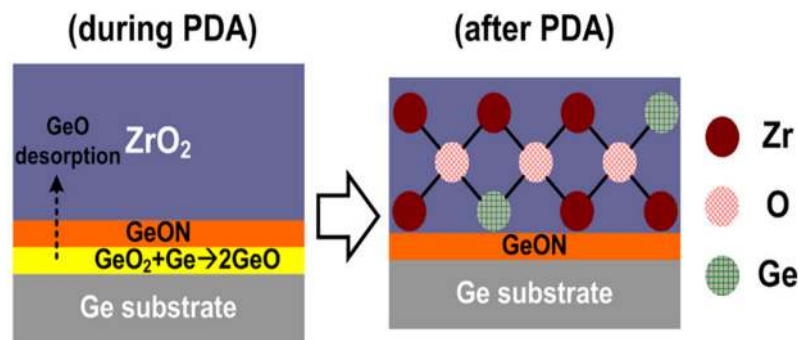


**Figure 8.** Nitriding treatment and  $\text{GeO}_2$  thermal decomposition into the  $\text{ZrO}_2$  layer to form a stable crystal state [78]. Reprinted from [78]; 2013 AIP Publishing.

Even so, how to reduce the leakage current density of the single crystalline  $\text{ZrO}_2$  layer is still a great challenge. At present, many studies will utilize novel gate stack structures such as  $t\text{-ZrO}_2/\text{Al}_2\text{O}_3$  [80],  $\text{ZrO}_2/\text{Ge}/\text{ZrO}_2/\text{Y}_2\text{O}_3$  [75] or the crystallized  $\text{ZrO}_2/\text{AlN}$  [50] buffer layer to further reduce the leakage current and density of interface states. As a gate dielectric layer, crystalline  $\text{ZrO}_2$  can significantly increase the carrier mobility and the transistor driving current with reduction of the equivalent capacitor thickness (CET) because of a high  $k$  value. The results demonstrate that the utility of crystalline  $\text{ZrO}_2$  is a favorable technique to improve the electrical properties and gate dielectric performances. It opens up a new way for the development of possible applications as charge storage capacitors for active matrix display devices with high- $k$  dielectric.

#### 4.5. Low-Temperature Solution Process

The sol–gel process has been widely reported as a result of low processing consumption, simple and flexible operation. However, the common disadvantage of the solution process is that a higher annealing temperature ( $\geq 400$  °C) is required to remove most of the solvents and impurities, and convert the precursors into dense oxide films [82] (Figure 9). The high-temperature annealing hinders the application of the plastic substrate in flexible electronic devices, and causes huge energy consumption. In recent years, due to the increasing demand for a low thermal budget and flexible electronic devices, the research on the low temperature annealing solution process has aroused extensive interest. Approaches including the sol–gel on chip process [83], high pressure annealing [84], aqueous solution [85], combustion [86,87], the light wave/microwave annealing method [88] and ultraviolet ozone irradiation [89,90] have been used to effectively reduce the processing temperature of oxide films prepared by the solution process. Our group developed an ink system for drop-on-demand (DOD) printing high performance  $\text{ZrO}_2$  film at a low temperature [91]. In particular, ultraviolet ozone (UVO) can be employed to prepare oxide TFTs in fully solution-processed at room temperature [92].  $\text{ZrO}_2$  films were prepared by spin coating of zirconium acetylacetonate ( $\text{ZrAcAc}$ ) precursors with high UV absorption (Figure 10). The report indicated that the film’s surface became significantly smooth and led to a reduction of the oxygen vacancy defects. Moreover, the analysis revealed it could effectively facilitate the formation of metal-oxygen (M–O) bonds with high  $k$  dielectric properties ( $k = 13$ ). It is found that the leakage current with UVO treatment at room temperature was significantly lower than that of  $\text{ZrO}_2$  films treated by annealing at high temperature (Figure 11). The development of low temperature solution technology has obtained the advantages of energy saving, simplicity and low

cost compared with the traditional vacuum process. It has a great application prospect in the facile low-temperature solution production of high-quality flexible oxide electronic devices.

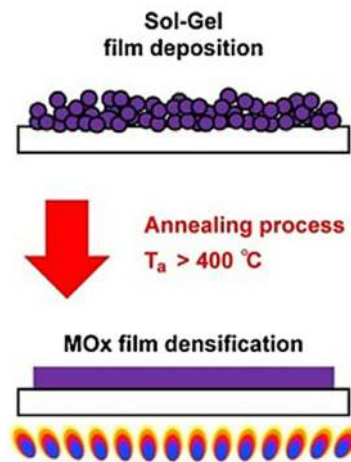


**Figure 9.** A schematic of densifying a sol–gel metal oxide film from as-spun xerogel via high-temperature thermal annealing [40]. Reprinted with permission from [40]; 2017 Elsevier.

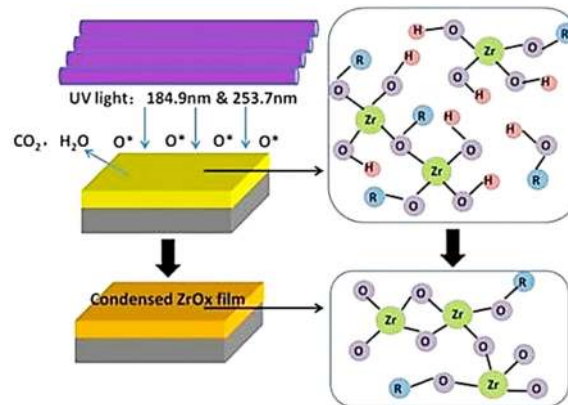


**Figure 10.** Schematic diagram of ZrAcAc sol–gel transformation mechanism under ultraviolet ozone (UVO) irradiation [92]. Reprinted with permission from [92]; 2017 Elsevier.

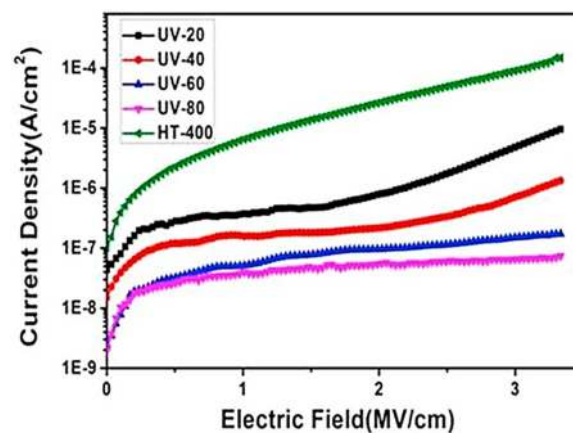


**Figure 11.** Comparison of leakage current in ZrO<sub>2</sub> films after annealing by UVO and high-temperature (HT) [92]. Reprinted with permission from [92]; 2017 Elsevier.

Table 1 shows the comparison of the properties of ZrO<sub>2</sub> and its optimized composite materials mentioned in this paper.

**Table 1.** Comparison of relevant properties of ZrO<sub>2</sub> and its composite material.

Material Structure	Leakage Current Density (A/cm <sup>2</sup> )	EOT (nm)	Carrier Mobility (cm <sup>2</sup> /V·s)	Density of States (eV <sup>-1</sup> cm <sup>-2</sup> )	k Value	Threshold Voltage (V)	Deposition Method	Application	Ref.
ZrO <sub>2</sub>	–	–	28	–	25	3.2	RF magnetron sputtering	TFT	[4]
N <sub>2</sub> + ZrO <sub>2</sub>	10 <sup>-9</sup> ~10 <sup>-8</sup>	–	22.5	7.06 × 10 <sup>12</sup>	–	0.1	EBE and PECVD	TFT	[35]
HfZrO <sub>2</sub>	3.6 × 10 <sup>-5</sup>	1.6~1.8	–	–	29~37	–	ALD	MIM	[62]
ZrO <sub>2</sub> /Si-N	–	1.6	–	5 × 10 <sup>12</sup>	11.5	–	ALD	MIM	[53]
ZrAlO	6.2 × 10 <sup>-7</sup>	19.3	40.6	3.30 × 10 <sup>12</sup>	19.67	0.71	ALD	FET	[57]
t-ZrO <sub>2</sub> /Al <sub>2</sub> O <sub>3</sub>	3.43 × 10 <sup>-5</sup>	1.09	–	3.35 × 10 <sup>11</sup>	21	–	Remote plasma ALD	MOS	[81]
PMMA-ZrO <sub>2</sub>	10 <sup>-6</sup> ~10 <sup>-5</sup>	–	0.48	–	4~12	3.3	Sol-Gel	TFT	[69]
Gd-ZrO <sub>2</sub>	1.8 × 10 <sup>-6</sup>	4.9	–	1.34 × 10 <sup>11</sup>	10.3	–	Sol-Gel	MOS	[61]
ZrHfO <sub>2</sub> -PMMA	7.7 × 10 <sup>-6</sup>	–	2.45	–	7.2~9.4	1.2	Sol-Gel	TFT	[66]
PMMA-ZrO <sub>2</sub>	3 × 10 <sup>-9</sup>	–	5.7 × 10 <sup>-2</sup>	7.5 × 10 <sup>10</sup>	–	0.8	EBE and Sol-Gel	OFET	[68]
Y-ZrO <sub>2</sub>	1.14 × 10 <sup>-7</sup>	0.67	68	1.2 × 10 <sup>12</sup>	30~33	–	co-sputtering	FET	[63]

## 5. Conclusions

In summary, ZrO<sub>2</sub> is one of the most promising materials to replace traditional SiO<sub>2</sub> and Si<sub>3</sub>N<sub>4</sub> dielectric layers due to its notably properties highlighting a (i) high dielectric constant, (ii) the capability of the room temperature process, (iii) high melting point, (iv) large band gap offset and (v) good thermal stability of contact with silicon and process compatibility. ZrO<sub>2</sub> and its optimized composite materials prepared by various deposition methods not only effectively reduced the leakage current and threshold voltage of the device, but also improved the on-to-off ratio of the device and the ability of the gate to control the current between the source and drain. It has great potential in CMOS and TFT devices and metal-insulator-metal (MIM) capacitor applications. However, there are still a series of problems to be solved to make it really practical. For example, the gate depletion effect of poly-Si will form a high resistance gate, and the interface mismatch between poly-Si gate and high k dielectric lead to the decrease of carrier mobility. The interface states caused by high k dielectric material will also cause a Fermi level pinning phenomenon, which leads to the shift of the gate voltage threshold and shows the need to find a suitable metal gate to replace the polysilicon gate electrode [24]. At the same time, the optimized and improved Zr-based films should conform to the trend of flexible, low-cost, low-temperature and printable electronic applications in the future.

The challenge that the new generation of scientists and engineers will face is not only to optimize and improve these new materials in the laboratory, but also to merge with the mature silicon process and Zr-based gate dielectric films in order to meet the requirements of the semiconductor industry. It can be expected that in the near future, the improved Zr-based and its composite gate dielectric films as high-k materials will first enter a practical stage in high-performance TFTs, and then will be used as the next generation of high-k materials in MOSFETs with the development and maturity of related technologies.

**Author Contributions:** Conceptualization, Z.Z. and J.X.; methodology, J.X.; validation, H.N., R.Y., H.T., J.P. and Z.Z.; formal analysis, Z.L. (Zhihang Li) and Z.L. (Zhihao Liang); investigation, J.X. and Z.Z.; resources, H.N., R.Y., Y.W. and S.Z.; data curation, J.X.; writing—original draft preparation, J.X. and Z.Z.; writing—review and editing, J.X., Z.Z., H.N., R.Y., J.P. and H.T.; supervision, H.N. and R.Y.; project administration, J.P.; funding acquisition, H.N. and R.Y. All authors have read and agreed to the published version of the manuscript.

**Funding:** This work was funded by Key-Area Research and Development Program of Guangdong Province (No. 2020B010183002 and No. 2019B010934001), National Natural Science Foundation of China (Grant No. 51771074 and 61574061), the Major Integrated Projects of National Natural Science Foundation of China (Grant No. U1601651), Guangdong Major Project of Basic and Applied Basic Research (No. 2019B030302007), Science and Technology Project of Guangzhou (No. 201904010344 and No. 201806010090), Fundamental Research Funds for

the Central Universities (No. 2019MS012), Ji Hua Laboratory scientific research project (X190221TF191) and the Open Project of Guangdong Province Key Lab of Display Material and Technology (No. 2017B030314031).

**Conflicts of Interest:** The authors declare no conflict of interest.

## References

1. Panda, D.; Tseng, T.-Y. Growth, dielectric properties, and memory device applications of ZrO<sub>2</sub> thin films. *Thin Solid Films* **2013**, *531*, 1–20. [[CrossRef](#)]
2. Wilk, G.D.; Wallace, R.M.; Anthony, J.M. High- $\kappa$  gate dielectrics: Current status and materials properties considerations. *J. Appl. Phys.* **2001**, *89*, 5243–5275. [[CrossRef](#)]
3. Chang, J.P.; Lin, Y.S. Dielectric property and conduction mechanism of ultrathin zirconium oxide films. *Appl. Phys. Lett.* **2001**, *79*, 3666–3668. [[CrossRef](#)]
4. Jae Sang, L.; Seongpil, C.; Sang-Mo, K.; Sang Yeol, L. High-Performance a-IGZO TFT With ZrO<sub>2</sub> Gate Dielectric Fabricated at Room Temperature. *IEEE Electron Device Lett.* **2010**, *31*, 225–227. [[CrossRef](#)]
5. Lee, S.Y.; Chang, S.; Lee, J.-S. Role of high-k gate insulators for oxide thin film transistors. *Thin Solid Films* **2010**, *518*, 3030–3032. [[CrossRef](#)]
6. Kol, S.; Oral, A. Hf-Based High- $\kappa$  Dielectrics: A Review. *Acta Phys. Pol. A* **2019**, *136*, 873–881. [[CrossRef](#)]
7. Robertson, J.; Wallace, R.M. High-K materials and metal gates for CMOS applications. *Mater. Sci. Eng. R Rep.* **2015**, *88*, 1–41. [[CrossRef](#)]
8. Yu, S.; Guan, X.; Wong, H.S.P. Conduction mechanism of TiN/HfO<sub>x</sub>/Pt resistive switching memory: A trap-assisted-tunneling model. *Appl. Phys. Lett.* **2011**, *99*, 063507. [[CrossRef](#)]
9. Ha, Y.G.; Everaerts, K.; Hersam, M.C.; Marks, T.J. Hybrid gate dielectric materials for unconventional electronic circuitry. *Acc Chem. Res.* **2014**, *47*, 1019–1028. [[CrossRef](#)]
10. Copel, M.; Gribelyuk, M.; Gusev, E. Structure and stability of ultrathin zirconium oxide layers on Si(001). *Appl. Phys. Lett.* **2000**, *76*, 436–438. [[CrossRef](#)]
11. Wong, Y.H.; Cheong, K.Y. ZrO<sub>2</sub> thin films on Si substrate. *J. Mater. Sci. Mater. Electron.* **2010**, *21*, 980–993. [[CrossRef](#)]
12. Jögi, I.; Kukli, K.; Ritala, M.; Leskelä, M.; Aarik, J.; Aidla, A.; Lu, J. Atomic layer deposition of high capacitance density Ta<sub>2</sub>O<sub>5</sub>–ZrO<sub>2</sub> based dielectrics for metal–insulator–metal structures. *Microelectron. Eng.* **2010**, *87*, 144–149. [[CrossRef](#)]
13. Vlček, J.; Rezek, J.; Houška, J.; Čerstvý, R.; Bugyi, R. Process stabilization and a significant enhancement of the deposition rate in reactive high-power impulse magnetron sputtering of ZrO<sub>2</sub> and Ta<sub>2</sub>O<sub>5</sub> films. *Surf. Coat. Technol.* **2013**, *236*, 550–556. [[CrossRef](#)]
14. Hwang, S.M.; Lee, S.M.; Park, K.; Lee, M.S.; Joo, J.; Lim, J.H.; Kim, H.; Yoon, J.J.; Kim, Y.D. Effect of annealing temperature on microstructural evolution and electrical properties of sol-gel processed ZrO<sub>2</sub>/Si films. *Appl. Phys. Lett.* **2011**, *98*, 022903. [[CrossRef](#)]
15. Zhao, X.; Vanderbilt, D. Phonons and lattice dielectric properties of zirconia. *Phys. Rev. B* **2002**, *65*, 075105. [[CrossRef](#)]
16. Vanderbilt, D.; Zhao, X.; Ceresoli, D. Structural and dielectric properties of crystalline and amorphous ZrO<sub>2</sub>. *Thin Solid Films* **2005**, *486*, 125–128. [[CrossRef](#)]
17. Lee, B.; Choi, K.J.; Hande, A.; Kim, M.J.; Wallace, R.M.; Kim, J.; Senzaki, Y.; Shenai, D.; Li, H.; Rousseau, M.; et al. A novel thermally-stable zirconium amidinate ALD precursor for ZrO<sub>2</sub> thin films. *Microelectron. Eng.* **2009**, *86*, 272–276. [[CrossRef](#)]
18. Yu, J.; Zhang, J.Y.; Boyd, I. Formation of stable zirconium oxide on silicon by photo-assisted sol-gel processing. *Appl. Surf. Sci.* **2002**, *186*, 190–194. [[CrossRef](#)]
19. Mih, T.A.; Paul, S.; Milanov, A.P.; Bhakta, R.; Devi, A. Capacitance-Voltage Analysis of ZrO<sub>2</sub> Thin Films Deposited by Thermal MOCVD Technique. *ECS Trans.* **2009**, *25*, 901–907. [[CrossRef](#)]
20. Hojabri, A. Structural and optical characterization of ZrO<sub>2</sub> thin films grown on silicon and quartz substrates. *J. Theor. Appl. Phys.* **2016**, *10*, 219–224. [[CrossRef](#)]
21. Kim, M.-S.; Ko, Y.-D.; Hong, J.-H.; Jeong, M.-C.; Myoung, J.-M.; Yun, I. Characteristics and processing effects of ZrO<sub>2</sub> thin films grown by metal-organic molecular beam epitaxy. *Appl. Surf. Sci.* **2004**, *227*, 387–398. [[CrossRef](#)]

22. Jena, S.; Tokas, R.B.; Thakur, S.; Sahoo, N.K. Optical properties of electron beam evaporated ZrO<sub>2</sub>:10% SiO<sub>2</sub> thin films: Dependence on structure. *Indian J. Phys.* **2016**, *90*, 951–957. [[CrossRef](#)]
23. Tang, W.T.; Ying, Z.F.; Hu, Z.G.; Li, W.W.; Sun, J.; Xu, N.; Wu, J.D. Synthesis and characterization of HfO<sub>2</sub> and ZrO<sub>2</sub> thin films deposited by plasma assisted reactive pulsed laser deposition at low temperature. *Thin Solid Films* **2010**, *518*, 5442–5446. [[CrossRef](#)]
24. Leskelä, M.; Niinistö, J.; Ritala, M. Atomic Layer Deposition. In *Comprehensive Materials Processing*; Elsevier: Amsterdam, The Netherlands, 2014; pp. 101–123. [[CrossRef](#)]
25. Niinistö, L.; Nieminen, M.; Päiväsaari, J.; Niinistö, J.; Putkonen, M.; Nieminen, M. Advanced electronic and optoelectronic materials by Atomic Layer Deposition: An overview with special emphasis on recent progress in processing of high-k dielectrics and other oxide materials. *Phys. Status Solid* **2004**, *201*, 1443–1452. [[CrossRef](#)]
26. Kukli, K.; Kemell, M.; Köykkä, J.; Mizohata, K.; Vehkamäki, M.; Ritala, M.; Leskelä, M. Atomic layer deposition of zirconium dioxide from zirconium tetrachloride and ozone. *Thin Solid Films* **2015**, *589*, 597–604. [[CrossRef](#)]
27. Hausmann, D.M.; Kim, E.; Becker, J.; Gordon, R.G. Atomic Layer Deposition of Hafnium and Zirconium Oxides Using Metal Amide Precursors. *Am. Chem. Soc.* **2002**, *14*, 4350–4358. [[CrossRef](#)]
28. Rossnagel, S.M. Thin film deposition with physical vapor deposition and related technologies. *J. Vac. Sci. Technol. A Vac. Surf. Films* **2003**, *21*, S74–S87. [[CrossRef](#)]
29. Baptista, A.; Silva, F.; Porteiro, J.; Míguez, J.; Pinto, G. Sputtering Physical Vapour Deposition (PVD) Coatings: A Critical Review on Process Improvement and Market Trend Demands. *Coatings* **2018**, *8*, 402. [[CrossRef](#)]
30. Khojier, K.; Savaloni, H.; Jafari, F. Structural, electrical, and decorative properties of sputtered zirconium thin films during post-annealing process. *J. Theor. Appl. Phys.* **2013**, *7*, 55. [[CrossRef](#)]
31. Patel, U.S.; Patel, K.H.; Chauhan, K.V.; Chawla, A.K.; Rawal, S.K. Investigation of Various Properties for Zirconium Oxide Films Synthesized by Sputtering. *Procedia Technol.* **2016**, *23*, 336–343. [[CrossRef](#)]
32. Prabakar, K.; Park, A.; Cho, N.; Lee, W.I.; Hwangbo, C.K.; Lee, J.G.; Lee, C. rf-Magnetron sputter deposited ZrO<sub>2</sub> dielectrics for metal–insulator–semiconductor capacitors. *Vacuum* **2008**, *82*, 1367–1370. [[CrossRef](#)]
33. Jones, A.C.; Hitchman, M.L. Chapter 1. Overview of Chemical Vapour Deposition. In *Chemical Vapour Deposition*; The Royal Society of Chemistry: Cambridge, UK, 2008; pp. 1–36.
34. Cabello, G.; Lillo, L.; Buono-Core, G.E. Zr(IV) and Hf(IV) β-diketonate complexes as precursors for the photochemical deposition of ZrO<sub>2</sub> and HfO<sub>2</sub> thin films. *J. Non-Cryst. Solids* **2008**, *354*, 982–988. [[CrossRef](#)]
35. Wu, C.H.; Huang, B.W.; Chang, K.M.; Wang, S.J.; Lin, J.H.; Hsu, J.M. The Performance Improvement of N<sub>2</sub> Plasma Treatment on ZrO<sub>2</sub> Gate Dielectric Thin-Film Transistors with Atmospheric Pressure Plasma-Enhanced Chemical Vapor Deposition IGZO Channel. *J. Nanosci. Nanotechnol.* **2016**, *16*, 6044–6048. [[CrossRef](#)] [[PubMed](#)]
36. Cárcamo-León, P.; Torres-Huerta, A.M.; Domínguez-Crespo, M.; Ramírez-Meneses, E. Synthesis of Transparent ZrO<sub>2</sub> Thin Films by MOCVD. *ECS Trans.* **2009**, *25*, 475–482. [[CrossRef](#)]
37. Karlsson, P.G.; Göthelid, E.; Richter, J.H.; Sandell, A. Initial stages of ZrO<sub>2</sub> chemical vapor deposition on Si(100)-(2×1) from zirconium tetra-tert-butoxide. *Surf. Sci.* **2008**, *602*, 1803–1809. [[CrossRef](#)]
38. Choy, K.L. Chemical vapour deposition of coatings. *Prog. Mater. Sci.* **2003**, *48*, 57–170. [[CrossRef](#)]
39. Xu, W.; Li, H.; Xu, J.B.; Wang, L. Recent Advances of Solution-Processed Metal Oxide Thin-Film Transistors. *ACS Appl. Mater. Interfaces* **2018**, *10*, 25878–25901. [[CrossRef](#)]
40. Park, S.; Kim, C.-H.; Lee, W.-J.; Sung, S.; Yoon, M.-H. Sol-gel metal oxide dielectrics for all-solution-processed electronics. *Mater. Sci. Eng. R Rep.* **2017**, *114*, 1–22. [[CrossRef](#)]
41. Van Elshocht, S.; Hardy, A.; Adelman, C.; Caymax, M.; Conard, T.; Franquet, A.; Richard, O.; Van Bael, M.K.; Mullens, J.; De Gendt, S. Impact of Process Optimizations on the Electrical Performance of High-k Layers Deposited by Aqueous Chemical Solution Deposition. *J. Electrochem. Soc.* **2008**, *155*, G91. [[CrossRef](#)]
42. Dutta, S.; Pandey, A.; Yadav, I.; Thakur, O.P.; Kumar, A.; Pal, R.; Chatterjee, R. Growth and electrical properties of spin coated ultrathin ZrO<sub>2</sub> films on silicon. *J. Appl. Phys.* **2013**, *114*, 014105. [[CrossRef](#)]
43. Aoki, Y.; Kunitake, T. Solution-based Fabrication of High-κ Gate Dielectrics for Next-Generation Metal-Oxide Semiconductor Transistors. *Adv. Mater.* **2004**, *16*, 118–123. [[CrossRef](#)]
44. Boratto, M.H.; Congiu, M.; dos Santos, S.B.O.; Scalvi, L.V.A. Annealing temperature influence on sol-gel processed zirconium oxide thin films for electronic applications. *Ceram. Int.* **2018**, *44*, 10790–10796. [[CrossRef](#)]
45. Ishii, H.; Kidera, T.; Nakajima, A.; Yokoyama, S. Atomic-layer deposition of ZrO<sub>2</sub> with a Si nitride barrier layer. *Appl. Phys. Lett.* **2002**, *81*, 2824–2826.



46. Lü, S.; Yin, J.; Xia, Y.; Gao, L.; Liu, Z. Study on the thermal stability and electrical properties of the high-k dielectrics  $(\text{ZrO}_2)_x(\text{SiO}_2)_{1-x}$ . *Sci. China Ser. E Technol. Sci.* **2009**, *52*, 2222–2226. [[CrossRef](#)]
47. Wilk, G.D.; Wallace, R.M. Stable zirconium silicate gate dielectrics deposited directly on silicon. *Appl. Phys. Lett.* **2000**, *76*, 112–114. [[CrossRef](#)]
48. Ouyang, L.; Ching, W.Y. Electronic structure and dielectric properties of dielectric gate material  $(\text{ZrO}_2)_x(\text{SiO}_2)_{1-x}$ . *J. Appl. Phys.* **2004**, *95*, 7918–7924. [[CrossRef](#)]
49. Puthenkovilakam, R.; Carter, E.A.; Chang, J.P. First-principles exploration of alternative gate dielectrics: Electronic structure of  $\text{ZrO}_2/\text{Si}$  and  $\text{ZrSiO}_4/\text{Si}$  interfaces. *Phys. Rev. B* **2004**, *69*, 155329. [[CrossRef](#)]
50. Wang, W.-C.; Tsai, M.-C.; Lin, Y.-P.; Tsai, Y.-J.; Lin, H.-C.; Chen, M.-J. Suppression of interfacial layer in high-K gate stack with crystalline high-K dielectric and AlN buffer layer structure. *Mater. Chem. Phys.* **2016**, *184*, 291–297. [[CrossRef](#)]
51. Jeon, S.; Choi, C.-J.; Seong, T.-Y.; Hwang, H. Electrical characteristics of  $\text{ZrO}_x\text{N}_y$  prepared by  $\text{NH}_3$  annealing of  $\text{ZrO}_2$ . *Appl. Phys. Lett.* **2001**, *79*, 245–247. [[CrossRef](#)]
52. Nieh, R.; Choi, R.; Gopalan, S.; Onishi, K.; Kang, C.S.; Cho, H.-J.; Krishnan, S.; Lee, J.C. Evaluation of silicon surface nitridation effects on ultra-thin  $\text{ZrO}_2$  gate dielectrics. *Appl. Phys. Lett.* **2002**, *81*, 1663–1665. [[CrossRef](#)]
53. Ishii, H.; Nakajima, A.; Yokoyama, S. Growth and electrical properties of atomic-layer deposited  $\text{ZrO}_2/\text{Si}$ -nitride stack gate dielectrics. *J. Appl. Phys.* **2004**, *95*, 536–542. [[CrossRef](#)]
54. Yana, G.; Xifeng, L.; Longlong, C.; Jifeng, S.; Xiao Wei, S.; Jianhua, Z. High Mobility Solution-Processed Hafnium Indium Zinc Oxide TFT With an Al-Doped  $\text{ZrO}_2$  Gate Dielectric. *IEEE Electron Device Lett.* **2014**, *35*, 554–556. [[CrossRef](#)]
55. Liang, Z.; Zhou, S.; Cai, W.; Fu, X.; Ning, H.; Chen, J.; Yuan, W.; Zhu, Z.; Yao, R.; Peng, J. Zirconium-Aluminum-Oxide Dielectric Layer with High Dielectric and Relatively Low Leakage Prepared by Spin-Coating and the Application in Thin-Film Transistor. *Coatings* **2020**, *10*, 282. [[CrossRef](#)]
56. Peng, J.; Wei, J.; Zhu, Z.; Ning, H.; Cai, W.; Lu, K.; Yao, R.; Tao, H.; Zheng, Y.; Lu, X. Properties-Adjustable Alumina-Zirconia Nanolaminate Dielectric Fabricated by Spin-Coating. *Nanomaterials* **2017**, *7*, 419. [[CrossRef](#)] [[PubMed](#)]
57. Song, X.; Xu, J.; Liu, L.; Deng, Y.; Lai, P.T.; Tang, W.M. Optimizing Al-doped  $\text{ZrO}_2$  as the gate dielectric for  $\text{MoS}_2$  field-effect transistors. *Nanotechnology* **2020**, *31*, 135206. [[CrossRef](#)] [[PubMed](#)]
58. Zhou, Y.; Liang, Z.; Yao, R.; Zuo, W.; Zhou, S.; Zhu, Z.; Wang, Y.; Qiu, T.; Ning, H.; Peng, J. Effect of Zirconium Doping on Electrical Properties of Aluminum Oxide Dielectric Layer by Spin Coating Method with Low Temperature Preparation. *Coatings* **2020**, *10*, 620. [[CrossRef](#)]
59. Zhang, J.; Ding, X.; Li, J.; Zhang, H.; Jiang, X.; Zhang, Z. Performance enhancement in  $\text{InZnO}$  thin-film transistors with compounded  $\text{ZrO}_2\text{-Al}_2\text{O}_3$  nanolaminate as gate insulators. *Ceram. Int.* **2016**, *42*, 8115–8119. [[CrossRef](#)]
60. Gholipur, R.; Bahari, A.; Ebrahimzadeh, M. Deposition of Nanostructured  $\text{Zr}_x\text{La}_{1-x}\text{O}_y$  Thin Films on P-type Si(100) Substrate by the Sol-Gel Route. *Silicon* **2015**, *9*, 173–181. [[CrossRef](#)]
61. Xiao, D.Q.; He, G.; Lv, J.G.; Wang, P.H.; Liu, M.; Gao, J.; Jin, P.; Jiang, S.S.; Li, W.D.; Sun, Z.Q. Interfacial modulation and electrical properties improvement of solution-processed  $\text{ZrO}_2$  gate dielectrics upon Gd incorporation. *J. Alloys Compd.* **2017**, *699*, 415–420. [[CrossRef](#)]
62. Bang, S.; Lee, S.; Jeon, S.; Kwon, S.; Jeong, W.; Kim, S.; Jeon, H. Physical and Electrical Properties of Hafnium-Zirconium-Oxide Films Grown by Atomic Layer Deposition. *J. Electrochem. Soc.* **2008**, *155*, H633–H637. [[CrossRef](#)]
63. Lee, T.I.; Ahn, H.J.; Kim, M.J.; Shin, E.J.; Lee, S.H.; Shin, S.W.; Hwang, W.S.; Yu, H.-Y.; Cho, B.J. Ultrathin EOT (0.67 nm) High-k Dielectric on Ge MOSFET Using Y Doped  $\text{ZrO}_2$  With Record-Low Leakage Current. *IEEE Electron Device Lett.* **2019**, *40*, 502–505. [[CrossRef](#)]
64. Jeong, J.W.; Hwang, H.S.; Choi, D.; Ma, B.C.; Jung, J.; Chang, M. Hybrid Polymer/Metal Oxide Thin Films for High Performance, Flexible Transistors. *Micromachines* **2020**, *11*, 264. [[CrossRef](#)] [[PubMed](#)]
65. Kim, G.H.; Yoon, S.-M.; Kang, S.Y.; Kim, C.A.; Ahn, S.D.; Suh, K.S. Organic field-effect transistors with thermal-cured polyacrylate gate dielectric films. *Thin Solid Films* **2008**, *516*, 1574–1577. [[CrossRef](#)]
66. Syamala Rao, M.G.; Pacheco-Zuñiga, M.A.; Garcia-Cerda, L.A.; Gutiérrez-Heredia, G.; Torres Ochoa, J.A.; Quevedo López, M.A.; Ramírez-Bon, R. Low-temperature sol-gel  $\text{ZrHfO}_2$ -PMMA hybrid dielectric thin-films for metal oxide TFTs. *J. Non-Cryst. Solids* **2018**, *502*, 152–158. [[CrossRef](#)]

67. Ha, Y.-g.; Jeong, S.; Wu, J.; Kim, M.-G.; Dravid, V.P.; Facchetti, A.; Marks, T.J. Flexible Low-Voltage Organic Thin-Film Transistors Enabled by Low-Temperature, Ambient Solution-Processable Inorganic/Organic Hybrid Gate Dielectrics. *J. Am. Chem. Soc.* **2010**, *132*, 17426–17434. [[CrossRef](#)] [[PubMed](#)]
68. Shang, L.; Liu, M.; Tu, D.; Liu, G.; Liu, X.; Ji, Z. Low-Voltage Organic Field-Effect Transistor With PMMA/ZrO<sub>2</sub> Bilayer Dielectric. *IEEE Trans. Electron Devices* **2009**, *56*, 370–376. [[CrossRef](#)]
69. Alvarado-Beltran, C.G.; Almaral-Sanchez, J.L.; Mejia, I.; Quevedo-Lopez, M.A.; Ramirez-Bon, R. Sol-Gel PMMA-ZrO<sub>2</sub> Hybrid Layers as Gate Dielectric for Low-Temperature ZnO-Based Thin-Film Transistors. *ACS Omega* **2017**, *2*, 6968–6974. [[CrossRef](#)]
70. Son, B.-G.; Je, S.Y.; Kim, H.J.; Jeong, J.K. Modification of a polymer gate insulator by zirconium oxide doping for low temperature, high performance indium zinc oxide transistors. *RSC Adv.* **2014**, *4*, 45742–45748. [[CrossRef](#)]
71. Hwang, J.; Lee, J.; Kim, Y.; Lee, E.; Wang, Y.; Kim, H. Hybrid gate insulator for OTFT using dip-coating method. *Curr. Appl. Phys.* **2011**, *11*, S154–S157. [[CrossRef](#)]
72. Gong, Y.; Zhao, K.; He, H.; Cai, W.; Tang, N.; Ning, H.; Wu, S.; Gao, J.; Zhou, G.; Lu, X.; et al. Solution processable high quality ZrO<sub>2</sub> dielectric films for low operation voltage and flexible organic thin film transistor applications. *J. Phys. D Appl. Phys.* **2018**, *51*, 115105. [[CrossRef](#)]
73. Kim, M.J.; Pak, K.; Choi, J.; Lee, T.I.; Hwang, W.S.; Im, S.G.; Cho, B.J. Ultrathin ZrO<sub>x</sub>-Organic Hybrid Dielectric (EOT 3.2 nm) via Initiated Chemical Vapor Deposition for High-Performance Flexible Electronics. *ACS Appl. Mater. Interfaces* **2019**, *11*, 44513–44520. [[CrossRef](#)] [[PubMed](#)]
74. Fischer, D.; Kersch, A. The effect of dopants on the dielectric constant of HfO<sub>2</sub> and ZrO<sub>2</sub> from first principles. *Appl. Phys. Lett.* **2008**, *92*, 012908. [[CrossRef](#)]
75. Wu, Y.-H.; Wu, M.-L.; Lyu, R.-J.; Wu, J.-R.; Chen, L.-L.; Lin, C.-C. Crystalline ZrO<sub>2</sub>-gated Ge metal-oxide-semiconductor capacitors fabricated on Si substrate with Y<sub>2</sub>O<sub>3</sub> as passivation layer. *Appl. Phys. Lett.* **2011**, *98*, 203502. [[CrossRef](#)]
76. Huang, J.-J.; Huang, L.-T.; Tsai, M.-C.; Lee, M.-H.; Chen, M.-J. Enhancement of electrical characteristics and reliability in crystallized ZrO<sub>2</sub> gate dielectrics treated with in-situ atomic layer doping of nitrogen. *Appl. Surf. Sci.* **2014**, *305*, 214–220. [[CrossRef](#)]
77. Tsipas, P.; Volkos, S.N.; Sotiropoulos, A.; Galata, S.F.; Mavrou, G.; Tsoutsou, D.; Panayiotatos, Y.; Dimoulas, A.; Marchiori, C.; Fompeyrine, J. Germanium-induced stabilization of a very high-k zirconia phase in ZrO<sub>2</sub>/GeO<sub>2</sub> gate stacks. *Appl. Phys. Lett.* **2008**, *93*, 082904. [[CrossRef](#)]
78. Lin, C.-M.; Chang, H.-C.; Wong, I.H.; Luo, S.-J.; Liu, C.W.; Hu, C. Interfacial layer reduction and high permittivity tetragonal ZrO<sub>2</sub> on germanium reaching ultrathin 0.39 nm equivalent oxide thickness. *Appl. Phys. Lett.* **2013**, *102*, 232906. [[CrossRef](#)]
79. Liu, H.; Han, G.; Xu, Y.; Liu, Y.; Liu, T.-J.K.; Hao, Y. High-Mobility Ge pMOSFETs With Crystalline ZrO<sub>2</sub> Dielectric. *IEEE Electron Device Lett.* **2019**, *40*, 371–374. [[CrossRef](#)]
80. Wu, Y.-H.; Chen, L.-L.; Lyu, R.-J.; Li, M.-Y.; Wu, H.-C. Tetragonal ZrO<sub>2</sub>/Al<sub>2</sub>O<sub>3</sub> Stack as High-κ Gate Dielectric for Si-Based MOS Devices. *IEEE Electron Device Lett.* **2010**, *31*, 1014–1016. [[CrossRef](#)]
81. Huang, J.-J.; Tsai, Y.-J.; Tsai, M.-C.; Lee, M.-H.; Chen, M.-J. Double nitridation of crystalline ZrO<sub>2</sub>/Al<sub>2</sub>O<sub>3</sub> buffer gate stack with high capacitance, low leakage and improved thermal stability. *Appl. Surf. Sci.* **2015**, *330*, 221–227. [[CrossRef](#)]
82. Wang, S.; Xia, G. A facile low-cost preparation of high-k ZrO<sub>2</sub> dielectric films for superior thin-film transistors. *Ceram. Int.* **2019**, *45*, 23666–23672. [[CrossRef](#)]
83. Banger, K.K.; Yamashita, Y.; Mori, K.; Peterson, R.L.; Leedham, T.; Rickard, J.; Siringhaus, H. Low-temperature, high-performance solution-processed metal oxide thin-film transistors formed by a ‘sol-gel on chip’ process. *Nat. Mater.* **2011**, *10*, 45–50. [[CrossRef](#)] [[PubMed](#)]
84. Kim, S.J.; Yoon, D.H.; Rim, Y.S.; Kim, H.J. Low-Temperature Solution-Processed ZrO<sub>2</sub> Gate Insulators for Thin-Film Transistors Using High-Pressure Annealing. *Electrochem. Solid-State Lett.* **2011**, *14*, E35. [[CrossRef](#)]
85. Hwan Hwang, Y.; Seo, J.-S.; Moon Yun, J.; Park, H.; Yang, S.; Ko Park, S.-H.; Bae, B.-S. An ‘aqueous route’ for the fabrication of low-temperature-processable oxide flexible transparent thin-film transistors on plastic substrates. *NPG Asia Mater.* **2013**, *5*, e45. [[CrossRef](#)]
86. Kim, M.G.; Kanatzidis, M.G.; Facchetti, A.; Marks, T.J. Low-temperature fabrication of high-performance metal oxide thin-film electronics via combustion processing. *Nat. Mater.* **2011**, *10*, 382–388. [[CrossRef](#)]

87. Wang, B.; Yu, X.; Guo, P.; Huang, W.; Zeng, L.; Zhou, N.; Chi, L.; Bedzyk, M.J.; Chang, R.P.H.; Marks, T.J.; et al. Solution-Processed All-Oxide Transparent High-Performance Transistors Fabricated by Spray-Combustion Synthesis. *Adv. Electron. Mater.* **2016**, *2*, 1500427. [[CrossRef](#)]
88. Xia, G.; Wang, S. Rapid and facile low-temperature solution production of ZrO<sub>2</sub> films as high-k dielectrics for flexible low-voltage thin-film transistors. *Ceram. Int.* **2019**, *45*, 16482–16488. [[CrossRef](#)]
89. Oluwabi, A.T.; Gaspar, D.; Katerski, A.; Mere, A.; Krunk, M.; Pereira, L.; Oja Acik, I. Influence of Post-UV/Ozone Treatment of Ultrasonic-Sprayed Zirconium Oxide Dielectric Films for a Low-Temperature Oxide Thin Film Transistor. *Materials* **2019**, *13*, 6. [[CrossRef](#)]
90. Gong, Y.; Zhao, K.; Yan, L.; Wei, W.; Yang, C.; Ning, H.; Wu, S.; Gao, J.; Zhou, G.; Lu, X.; et al. Room Temperature Fabrication of High Quality ZrO<sub>2</sub> Dielectric Films for High Performance Flexible Organic Transistor Applications. *IEEE Electron Device Lett.* **2018**, *39*, 280–283. [[CrossRef](#)]
91. Zhu, Z.; Zhang, J.; Zhou, Z.; Ning, H.; Cai, W.; Wei, J.; Zhou, S.; Yao, R.; Lu, X.; Peng, J. A Simple, Low Cost Ink System for Drop-on-Demand Printing High Performance Metal Oxide Dielectric Film at Low Temperature. *ACS Appl. Mater. Interfaces* **2019**, *11*, 5193–5199. [[CrossRef](#)]
92. Dong, X.; Xia, G.; Zhang, Q.; Li, L.; Gong, H.; Bi, J.; Wang, S. Room-temperature UV-ozone assisted solution process for zirconium oxide films with high dielectric properties. *Ceram. Int.* **2017**, *43*, 15205–15213. [[CrossRef](#)]



© 2020 by the authors. Licensee MDPI, Basel, Switzerland. This article is an open access article distributed under the terms and conditions of the Creative Commons Attribution (CC BY) license (<http://creativecommons.org/licenses/by/4.0/>).